A comprehensible study of ionization efficiency for pure crystals, LAr and LXe ionization detectors.[1]

CCD's and TPC's

Youssef Sarkis

ICN-UNAM

Fermilab Early Career Seminar Series

[1]Based on: Phys. Rev. D 101, 102001 –Published 1 May 2020

Contents

A little about me

PhD graduate in physical sciences at Instituto de Ciencias Nucleares UNAM. My principal mentor is Alexis A. Aguilar Arévalo.

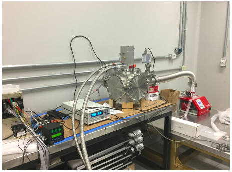

- I began my career as an experimental particle physics at ICN-UNAM.
- I have worked with PMT and high voltage supplies.
- As an undergrad I worked in direct dark matter (DM) searches as part of DAMIC.
- I learned about background characterization for DM experiments.
- I also worked in CEνNS physics and phenomenology as part of CONNIEs.
- One way or another these lead me to study the theory of ionization efficiency.
- Now, I'm looking for a postdoc.

Fermilab fellow experience

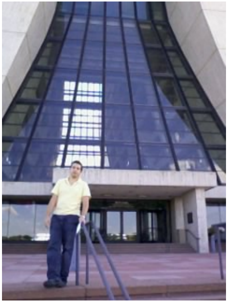

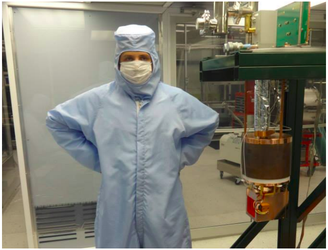

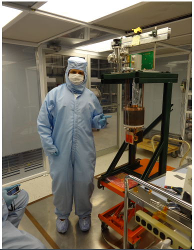

- Summer undergrad intern (2011) in D0 analyzing data for Higgs searches in the channel $WWW \to lv - jj - jj$.
- I worked in Sidet in the first CONNIE scientific tests.
- I learned about scientific grade CCD's developed in SiDet. Technical operations, software tests, and calibrations.
- Also in the assembling of the experiment in a clean room.
- I have also been in Fermilab for meetings of the collaboration.

Introduction: Dark Matter, CEνNS and Other Exotic Physical Process detections.

Challenge

One of the main challenges to detect Dark Matter (DM), CEνNS, etc, is to understand ionization coming from inter-atomic physics at low energies.

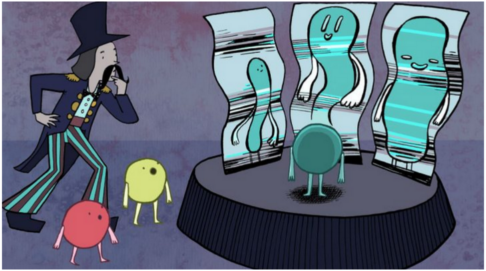

Credit: Symmetry Magazine/Sandbox Studio, Chicago

Dark Matter, indirect evidence and observations

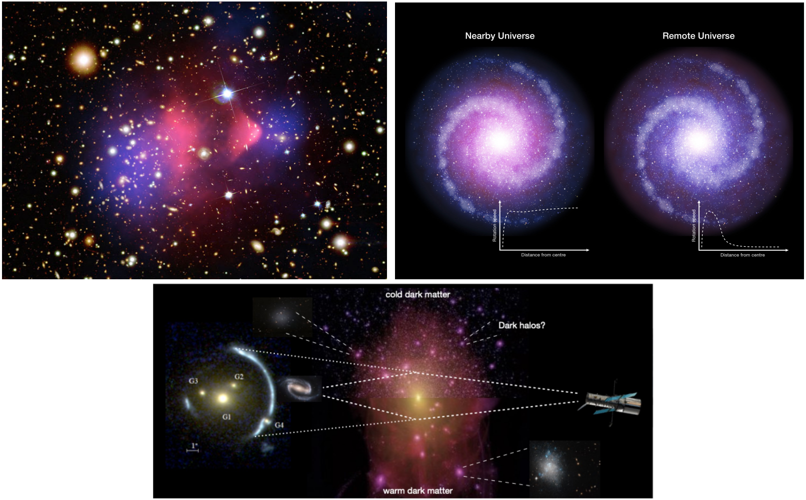

Figure: X-Ray:NASA/CXC/Cfa/M.Markevitch et al. NASA/ESA HST (strong lens, dwarf galaxies), M. Lovell (CDM/WDM simulations). Simulation source code is available at `http://beltoforion.de/galaxy/galaxy_en.html`

Detection Strategies

Credit:Institute of High Energy Physics, CAS,BI Xiaojun

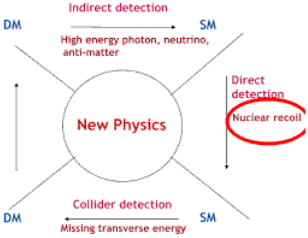

- WIMP's scatter nuclei give an exponential nuclear recoil (NR) spectrum.
- Hence a lower threshold will increase the rate.
- But what we detect is ionization signals generated by NR.

XENON100 Collaboration

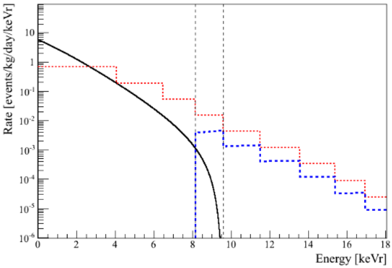

Figure: NR spectrum expected in Xe for a WIMP of 10 GeV$/c^2$ and cross section of 10^{-41} cm^2.

Relevant DM Experiments

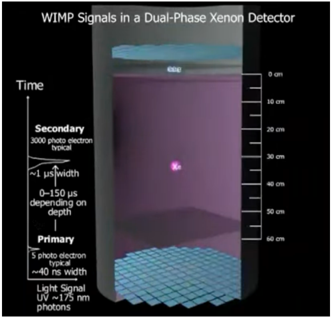

- TPC's detectors: LUX, XeNT, ZEPLIN, etc.
- Bolometers: Super CDMS, EDELWEISS, etc.
- CCD's: DAMIC and OSCURA.

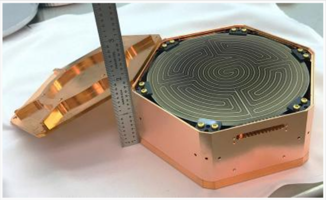

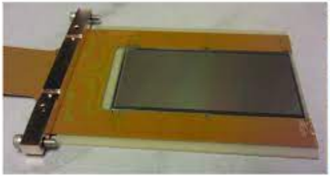

These detectors detect signals by ionization due to WIMP's that produce NR's in the material.

Figure: Credit images:M. Szydagis 2021 SCU AAP Conference https://damicm.cnrs.fr/en/detector/, https://supercdms.slac.stanford.edu/overview

Dark Matter Limits

- Direct Dark Matter detection are limited by the neutrino floor.
- Here also the ionization efficiency plays a crucial role.

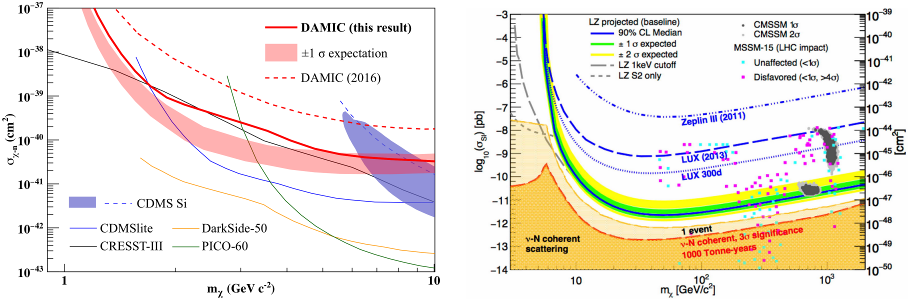

Figure: Phys. Rev. Lett. 125, 241803 (2020) and Phys. Rev. D 101, 052002 (2020)

CEνNS

Coherent elastic Neutrino Nuclear Scattering[2]

Neutral-current interaction where a neutrino of any flavor scatters off a nucleus as a whole.

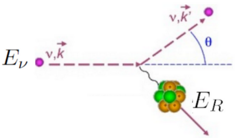

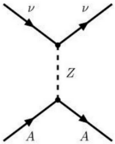

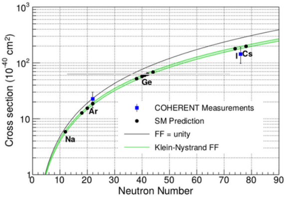

Weak nuclear charge $Q_W^2 \sim N^2$

$$\frac{d\sigma_{SM}}{dE_R}(E_{\bar{\nu}_e}) = \frac{G_F^2}{4\pi}\left[N - (1 - 4\sin^2\theta_W)Z\right]^2 \left(1 - \frac{ME_R}{2E_{\bar{\nu}_e}^2} - \frac{E_R}{E_{\bar{\nu}_e}} + \frac{E_R^2}{2E_{\bar{\nu}_e}^2}\right) MF^2(q)$$

First observed by the COHERENT Collaboration with neutrinos of E~16-53 MeV with a CsI detector (Science 357, 1123, 2017), and a Liquid Ar detector (PRL, 126, 012002, 2021).

Observation at lower energies (Reactors) may hint at Physics BSM.

[2] D.Z. Freedman, Coherent effects of a weak neutral current, Phys. Rev. D 9 (1974) 1389.

CEνNS Constrains Direct DM Searches.

Solar neutrinos are the ultimate background for direct DM experiments.

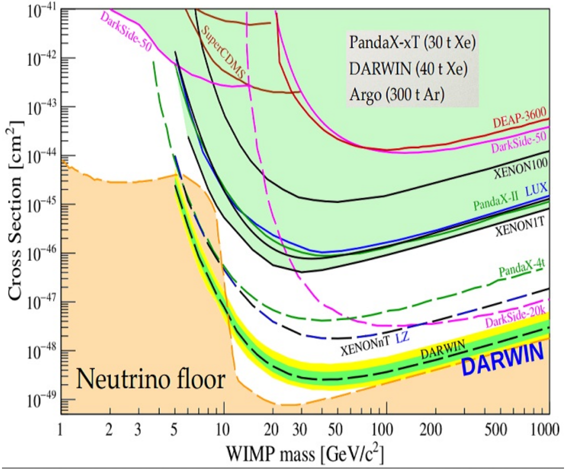

Figure: D20190401 aspen indico cern ch event 748043 c 3325970 neutrino floor dark matter.

Relevant Experiments

- CCD's: CONNIE.
- Ge detectors: CoGeNT, TEXONO, νGeN , CONUS.
- Low-temp. bolometers: RICOCHET, MINER, ν-cleus.
- Noble liquid detectors: LAr Livermore, LXe, ITEP& INR, LXe ZEPLIN-III.
- Neutron Spallation: COHERENT.

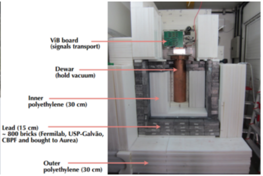

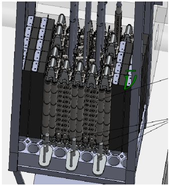

CAPTAIN – "Cryogenic Apparatus for Precision Tests of Argon Interactions with Neutrinos"

COHERENT SNS

https://coherent.ornl.gov/,Coherent Captain Mills: The Search for Sterile Neutrinos Ashley Elliott et al, https://indico.cern.ch/event/MINER_MI_workshop.pdf,http://icra.cbpf.br/twiki/bin/login/CONNIE

Ionization Efficiency; the Challenge of Low Energy Detection.

Ionization energy from nuclear recoils

- As for high energy physics, the Bethe-Bloch ionization formula is mandatory to reconstruct energy deposited in the detector.
- In this regime (III) all energy goings to ionization.

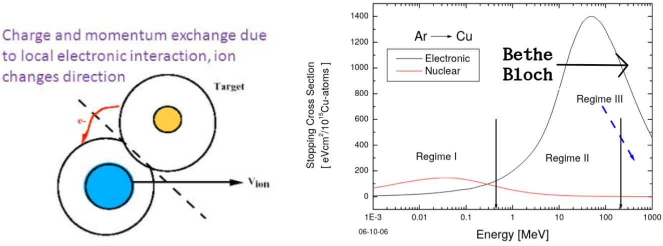

Figure: Credit:Ion implantation,by Moses Cobb and https://cds.cern.ch/record/1047064/files/p169.pdf

- For low energies ions (<10 MeV), nuclear stopping is comparable to electronic stopping.
- Hence in these regimes (I and II) not all the energy goes to ionization.

Ionization Efficiency

To start the cascade of recoiling atoms the particle,e.g χ, ν, have to deposit an energy grater than the Frenkel-pair energy (≈ 30 eV).

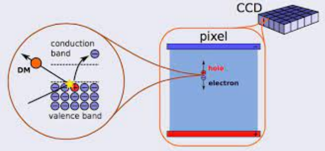

Deposited energy splits in;

E_ν : Nuclear collisions[3]. ($\bar{\nu}$)

E_I : Ionization (visible) energy $[\mathrm{keV_{ee}}]$ ($\bar{\eta}$).

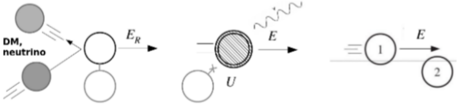

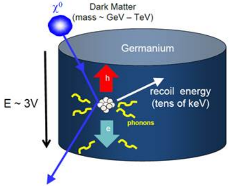

- $quenching = \frac{\text{total ionization energy}}{\text{total deposited energy}} = \boxed{f_n = \frac{\bar{\eta}}{\varepsilon_R}}$.
- $\varepsilon_R = \bar{\eta} + \bar{\nu}$, where ε_R is the recoil energy.
- Energy u is lost to some disruption of the atomic bonding: $\varepsilon_R = \varepsilon + u$.
- This sets a dissipative cascade of slowing-down processes

[3]Using dimensionless units ($\varepsilon = 16.26E(\mathrm{keV})/\mathrm{Z_1 Z_2}(\mathrm{Z_1^{0.23}} + \mathrm{Z_2^{0.23}})$)

Recoil Spectrum

As experiments have lowered their detection thresholds well below 1 keV, understanding the quenching at those low energies have become important.

$E_v = f_n(E_R)E_R$ be the visible energy.

The visible energy spectrum is shifted to lower energies, due to the QF,

$$\frac{dR}{dE_R} = \frac{dR}{dE_v}\frac{dE_v}{dE_R} = \frac{dR}{dE_v}\left(f_n + E_R\frac{df_n}{dE_R}\right)^-$$

*QF moves events below the threshold.

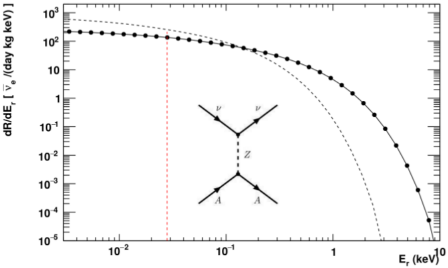

Figure: CEνNS spectrum $\frac{dR}{dE_v}$ (dotted) and $\frac{dR}{dE_R}$ (solid).

Physical Motivation

Physics Scope for CEνNS Experiments

1. CEνNS detection has motivated theoretical activity in high-energy physics.
2. Inspiring new constraints on beyond the Standard Model.

- Standard Model weak mixing angle.
- Non Standard Interactions (NSI) of neutrinos.
    - Dark Photons.
    - Anomalous magnetic moment.
    - neutrino anapole.
- Sterile oscillations.
- Neutron form factor.

J.HEP 2022 127 (2022)

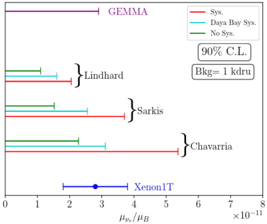

μ_B constraints & yields for solar ν studies

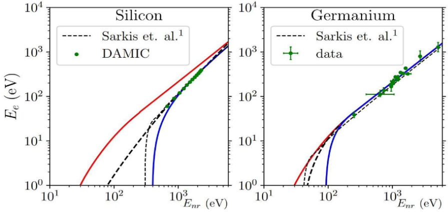

PRD 106 015002 (2022)

NSI; Vector and Axial-vector Interactions

- Higher-dimensional Lagrangian effective operators.

$$\mathcal{L}_{\mathrm{NSI}} \supset -2\sqrt{2}G_F \sum_{\alpha,\beta} \sum_{P,q} \epsilon_{\alpha\beta}^{q,P} \left(\bar{v}_\alpha \gamma^\mu P_L v_\beta\right) \left(\bar{q}\gamma_\mu P q\right) \quad (1)$$

- CEνNS experiments are primarily sensitive to light vector and scalar mediator models.

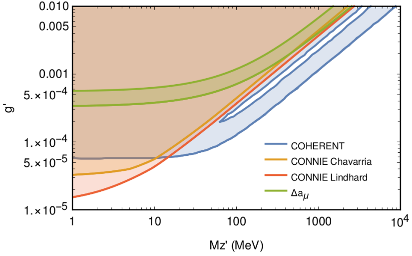

Figure: JHEP04(2020)054

SM Precision Tests

- From a phenomenological perspective, NSI may show up as a modification of $\sin^2(\theta_W)$ that is experimentally measured.
- This defines a scheme to compare the sensitivity of CEνNS experiments to other SM precision tests.
- A need to revisit low energy (ideal) analysis by including a realistic model for ionization efficiency.

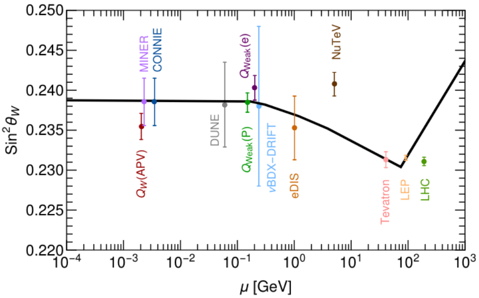

Figure: PRD 104, 033004 (2021)

Integral Equations Governing Ionization Process For Pure Crystals

Electronic Stopping Power

❁ The electronic stopping power S_e is the electronic friction (energy loss per unit length) that an ion feels when it is moving in a medium.

❁There are several models to compute this quantity, Lindhard used the dielectric function formalism. He deduce $\boldsymbol{S_e \propto E^{1/2}}$.

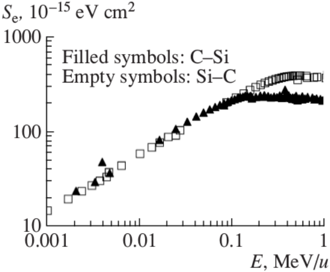

Figure: C-Si electronic stopping power, Sigmund, P. Stopping of slow ions.

General remarks:

- Excitation or ionization of target particles.
- Changes in the internal state of the projectile.
- Emission of radiation.

Nuclear Stopping Power

- The collision between two atoms, and can be described by classical kinematics.

- The projectile in the medium can hit a target ion transferring some of its energy.

- These define the nuclear stopping power S_n, related to elastic collisions due to an inter-atomic potential, defining also the nuclear cross section σ_n.

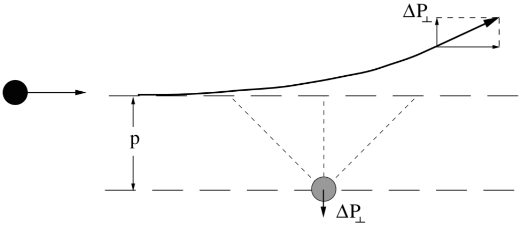

Figure: $V = \frac{e^2 F(r)}{r}$,F is an screening function,
`https://www.iue.tuwien.ac.at/phd/hoessinger/node4.html`

Basic Integral Equation and Approximations

(T_n : Nuclear kinetic energy and T_{ei} electron kinetic energy.)

$$\underbrace{\int d\sigma_{n,e}}_{\text{total cross section}} \left[\underbrace{\bar{\nu}\left(E - T_n - \sum_i T_{ei}\right)}_{\text{A}} + \underbrace{\bar{\nu}\left(T_n - U\right)}_{\text{B}} + \underbrace{\bar{\nu}(E)}_{\text{C}} + \underbrace{\sum_i \bar{\nu}_e\left(T_{ei} - U_{ei}\right)}_{\text{D}} \right] = 0 \qquad (2)$$

Lindhard's (five) approximations

1. Neglect contribution to atomic motion coming from electrons.
2. **Neglect the binding energy, U = 0. (Now taken into account)**
3. Energy transferred to electrons is small compared to that transferred to recoil ions.
4. Effects of electronic and atomic collisions can be treated separately.
5. T_n is also small compared to the energy E.

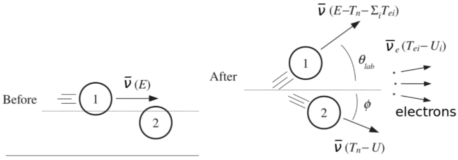

Elastic Scattering Parametrization

- In order to simplify Eq.(2), Lindhard assumed elastic scattering through the variable $t = \varepsilon^2 \sin^2(\theta/2)$ (magic variable).

- Nuclear cross section is: $d\sigma_n = \frac{f(t)}{2t^{3/2}} dt$, where $f(t)$ is a function related to the inter-atomic potential.

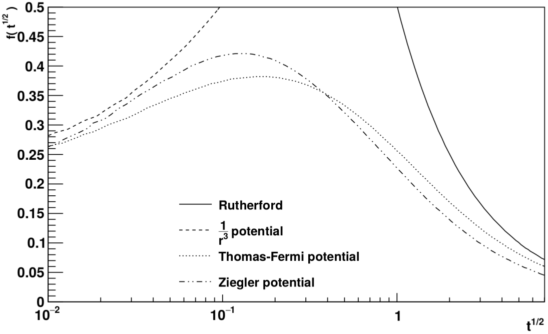

Figure: Screening function

Lindhard Simplified Equation

Using the five approximations Lindhard deduced an integral simplified equation,

$$\underbrace{\left(k\varepsilon^{1/2}\right)}_{S_e}\bar{\nu}'(\varepsilon) = \int_0^{\varepsilon^2} \underbrace{dt\frac{f\left(t^{1/2}\right)}{2t^{3/2}}}_{d\sigma_n}\left[\bar{\nu}(\varepsilon - t/\varepsilon) + \bar{\nu}(t/\varepsilon) - \bar{\nu}(\varepsilon)\right], \qquad (3)$$

L.H.S R.H.S

---

but since binding energy was neglected is only valid at high energies, since $\bar{\nu}(\varepsilon \to 0) \to \varepsilon$, by the above equation we get $\bar{\nu}'(0) = 0$!

- First principles elec. stop. power $S_e = k\varepsilon^{1/2}$, $k = 0.133Z^{2/3}/A^{1/2}$.
- Lindhard deduce a parametrization valid at high energies (U=0).
- But fails below 4 keV.

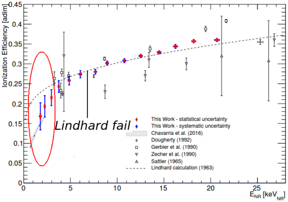

PRD Chavarria et all, 94, 082007(2016)

$$\bar{\nu}_L(\varepsilon) = \frac{\varepsilon}{1 + kg(\varepsilon)}, \; g(\varepsilon) = 3\varepsilon^{0.15} + 0.7\varepsilon^{0.6} + \varepsilon.$$

Lindhard QF and Other Works

- Lindhard used a primitive computer(DASK).
- His formula just solved approximately Eq. (3).

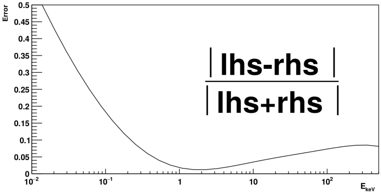

- Using Lindhard formula $\Rightarrow$ Systematic error, large at lower energies.
- Other authors [4], try to include binding energy.
- But fail to realize in changing the integration limit, reporting nonphysical results.
- One of the achievements of this work is to include in a consistent mathematical and physical way the binding energy.

[4] PHYSICAL REVIEW D 91, 083509 (2015)

Lindhard Approximations With Binding Energy.

In order to compute a solution for $\bar{\nu}$ that includes the binding energy, we make the following

1. Neglect atomic movement from electrons, since is negligible at low energies $\bar{\nu}_e = 0$.
2. Energy transferred to ionized electrons is small compared to that transferred to recoiling ions.
3. Effects of electronic and atomic collisions can be treated separately.
4. T_n is also small compared to the energy E.
5. Expand the terms in Eq. 2 up to **second order** in $\boxed{\Sigma_i T_{ei}/(E - T_n)}$.

The first four approximations are still the same that Lindhard used.

Second order expansion

In order to have a solvable equation at low energies we have to expand the term $\bar{\nu}\left(E - T_n - \Sigma_i T_{ei}\right)$ up to second order,

$$\begin{aligned}\bar{\nu}\left(E - T_n - \Sigma_i T_{ei}\right) \approx & \bar{\nu}\left(E - T_n\right) - \bar{\nu}'(E)\left(\Sigma_i T_{ei}\right) \\ & + \bar{\nu}''(E) T_n \left(\Sigma_i T_{ei}\right)\end{aligned} \tag{4}$$

this leads to the appearance of the electronic stopping power in the first derivative term

$$\int d\sigma_{n,e} \bar{\nu}'(E)\left(\Sigma_i T_{ei}\right) = \bar{\nu}'(E) S_e(\varepsilon), \quad \int d\sigma_e \left(\Sigma_i T_{ei}\right) = S_e(\varepsilon). \tag{5}$$

For the second derivative term, we can apply the integral mean value theorem

$$\int d\sigma_{n,e} \bar{\nu}''(E) T_n \left(\Sigma_i T_{ei}\right) = \bar{\nu}''(E) < T_n > S_e(\varepsilon). \tag{6}$$

Simplified Integral Equation With Binding Energy

A previous work[a] didn't notice the necessity to change the lower limit of integration in order to be consistent with the term $\bar{\nu}(t/\varepsilon - u)$. In our publication, we take this into account so Eq.2 becomes:

$$\boxed{-\frac{1}{2}k\varepsilon^{3/2}\bar{\nu}''(\varepsilon)} + \underbrace{k\varepsilon^{1/2}}_{S_e}\bar{\nu}'(\varepsilon) = \int_{\boxed{\varepsilon u}}^{\varepsilon^2} \underbrace{dt\frac{f\left(t^{1/2}\right)}{2t^{3/2}}}_{d\sigma_n}\left[\bar{\nu}(\varepsilon - t/\varepsilon) + \bar{\nu}(t/\varepsilon - \boxed{u}) - \bar{\nu}(\varepsilon)\right] \quad (7)$$

This equation can be solved numerically from $\varepsilon \geqslant u$. The equation predicts a threshold energy of u ($\varepsilon_R^{threshold} = 2u$).

The equation admits a solution featuring a "kink" at $\varepsilon = u$ (discontinuous 1st derivative). We assume that the binding energy is a constant $u = u_0$

[a] PhysRevD 91 083509 (2015)

Numerical Solution

We first notice that the QF depends only of $\boldsymbol{k}$ and $\boldsymbol{u}$.

Shooting method

We have the boundary condition (BC) $\bar{\nu}''(\varepsilon \to \infty) \to \mathbf{0}$.
Now, since the R.H.S of Eq. 7 is zero at $\varepsilon = \boldsymbol{u}$ and lower, we impose that the L.H.S to be zero at this point, this gives the relation

$$\alpha_1 = 1 + \frac{1}{2} u_0 \alpha_2$$

So we give an initial try of α_2 to hit the BC, we shoot in this way until the BC is satisfied.

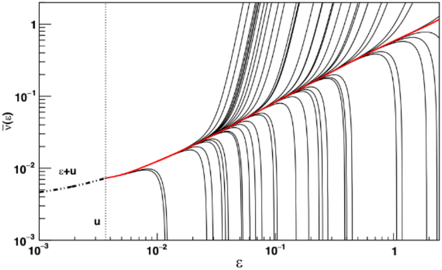

First results for Si

- The high energy cutoff is due to the limitations of the constant binding energy model.

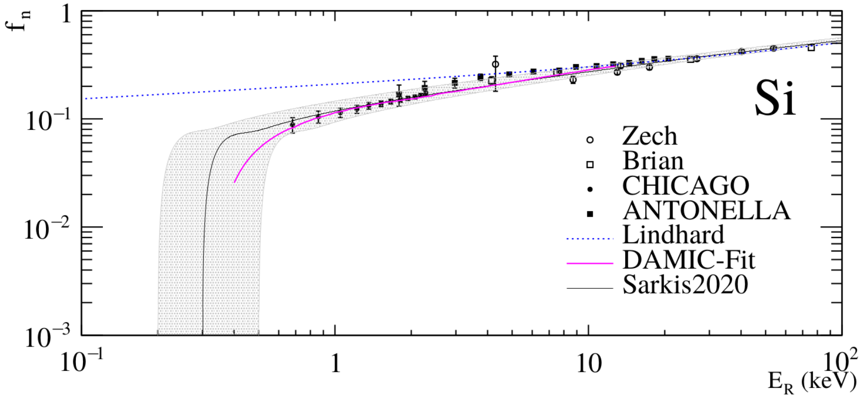

Figure: QF measurements for Si, compared with Lindhard model, the ansatz, and the numerical solution; $U = 0.15$ keV y $k = 0.161$.

Ge with recent data.

Results (Band is build to cover data)

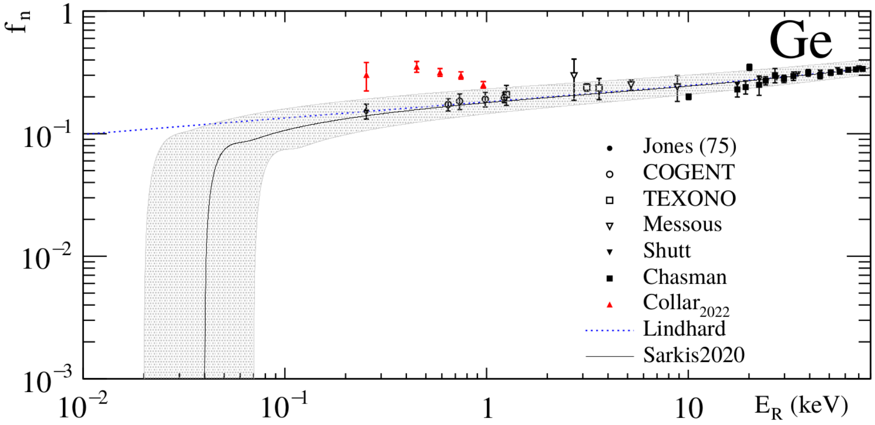

Figure: QF measurements for Ge, compared with Lindhard model, the ansatz, and the numerical solution; U = 0.02 keV y k = 0.162.

The Model in the Experimental Community

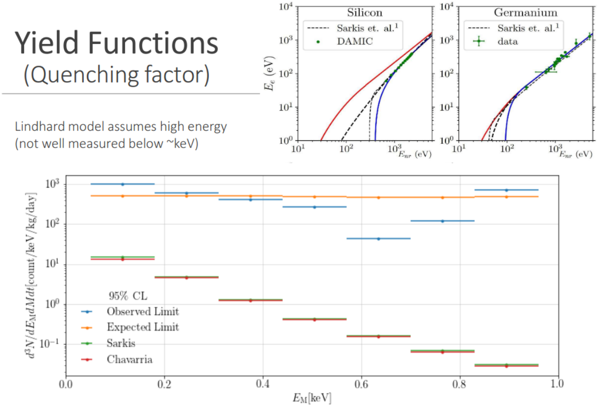

Figure: (Up) Tom Schwemberger (Univ. Oregon) talk at Mag.CEVNS2021. (Down) Reactor ON-OFF for CONNIE (1x5) 2022.

Improvements of the Model

- **For Si, constant U, gives a cut off too high compared to the expected threshold given by the energy to create a Frenkel-pair (≈ 30 eV).**
- A varying binding energy model is proposed;
  - Low energies just considered the Frenkel energy.
  - High energy consider electron inner excitations, using T.F theory.
- **Lindhard electronic stopping is not valid at low energies.**
- It doesn't considered Coulomb repulsion effects and electron stripping.
- We can also add electronic straggling $\Omega^2 = \langle \delta E - \langle \delta E \rangle \rangle^2$ ($\frac{d\Omega^2}{d\rho} \equiv W$) effects to the model.

$$\boxed{\begin{aligned} -\frac{1}{2}\varepsilon S_e(\varepsilon)\left(1+\frac{W(\varepsilon)}{S_e(\varepsilon)\varepsilon}\right)\bar{\nu}''(\varepsilon) + S_e(\varepsilon)\bar{\nu}'(\varepsilon) = \\ \int_{\varepsilon u}^{\varepsilon^2} dt \frac{f\left(t^{1/2}\right)}{2t^{3/2}}[\bar{\nu}(\varepsilon - t/\varepsilon) + \bar{\nu}(t/\varepsilon - u) - \bar{\nu}(\varepsilon)], \end{aligned}} \tag{8}$$

Low Energy Effects for Electron Gas (Scaling)

- Lindhard needed to add $\xi_e \approx Z^{1/6}$ to S_e for explain experimental data[5].
- Density Functional Theory (DFT) is used to estimate S_e and U.
- Usually the average Fermi energy $\frac{3}{5}E_F$, valid only at high energies.
- For low energies [6], due to Pauli exclusion principle, just electrons near E_F could be excited, $\frac{3}{5}E_F \rightarrow E_F$.
- Implies scaling $a = 0.885a_0/Z^{1/3}$ by $\frac{5}{3}$.
- With this $S_e \rightarrow \xi_e S_e$, $\xi_e = (5/3)^{3/2}$. **Hence for a wide range of energies ξ_e can vary among 1.0 and $(5/3)^{3/2} \approx$ 2.15.**
- Now we can understand the origin for ξ_e from DFT as a consequence of considering Pauli principle. Scaling also affects U and W.

[5] Included in the Lindhard formula for k $= 0.133Z^{2/3}A^{-1/2} = 0.133\xi_e(Z/A)^{-1/2}$.
[6] I. S. Tilinin Phys. Rev. A 51, 3058, 1 April 1995

High Energy Effects (> 10 keV) for $S_e(\varepsilon)$

§ *Bohr Stripping*

- Electrons can be lost according to momentum transferred.
- The effective number of electrons obeys $Z^\dagger \approx Z e^{-v/Z^{2/3} v_0}$.
- $S_e \propto Z^\dagger$, this leads to damping.

§ *Z Oscillations*

- When the ion charge changes, the transport cross section σ_T changes.
- Phase shift is appear to maintain neutrality of electron Fermi gas.
- S_e may be affected by this effect at energies $v \ll v_0 Z^{2/3}$.Since $S_e \propto \sigma_T$.

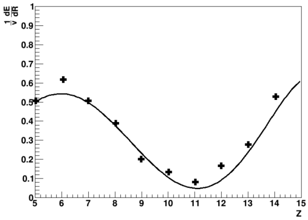

▫ Z oscillation for Si.

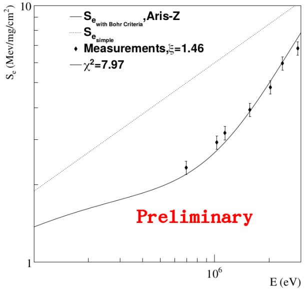

▫ S_e vs data

Low Energy Effects for S_e

§ *Coulomb repulsion effects*

- At low energies S_e departures from velocity proportionality.
- Colliding nuclei will partially penetrate the electron clouds.

$$S_e = (\Xi) N m v \int_0^\infty v_F \sigma_{tr}(v_F) N_e dV \to (\Xi) N m v \int_R^\infty v_F \sigma_{tr}(v_F) N_e dV$$

R distance closest approach and Ξ is a geometrical factor[4] , negligible for $Z < 20$.

- Three models will be considered; **Tilinin[7], Kishinevsky[8] and Arista[9]**
- Models change details of the inter-atomic potential.
- Hence affect $f(t^{1/2})$ and S_e at low energies.

---

[7] I.S.Tilinin Phys. Rev. A 51, 3058 (1995)

[8] Kishinevsky, L.M., 1962, Izv. Akad. Nauk SSSR, Ser. Fiz. 26, 1410.

[9] J.M. Fernández-Varea, N.R. Arista, Rad. Phy. and C.,V 96, 88-91, (2014),

Binding energy model

The model consider:

- Frenkel pair creation energy, U_{FP}.
- Atomic binding with DFT theory, $U_{TF}(E)$.
- $U(E) = U_{FP} + U_{TF}(E)$

$$U_{FP} = 23.54^{+9.63}_{-12.04}\ \text{eV}$$

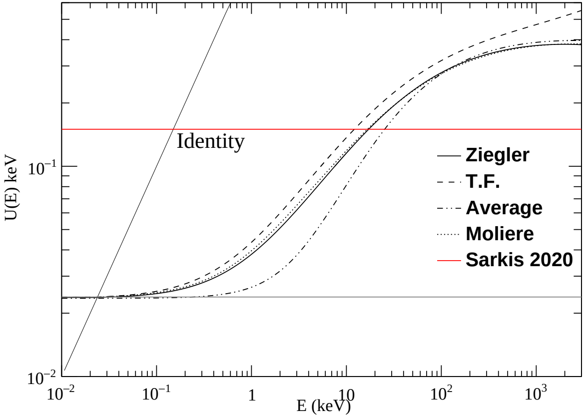

The DFT depends on the screening function used in the inter-atomic potential.

QF Results (Si) up to 3 MeV.

We fit the inter-atomic scale parameter, that scales S_e, S_n and has important effects at low energies.

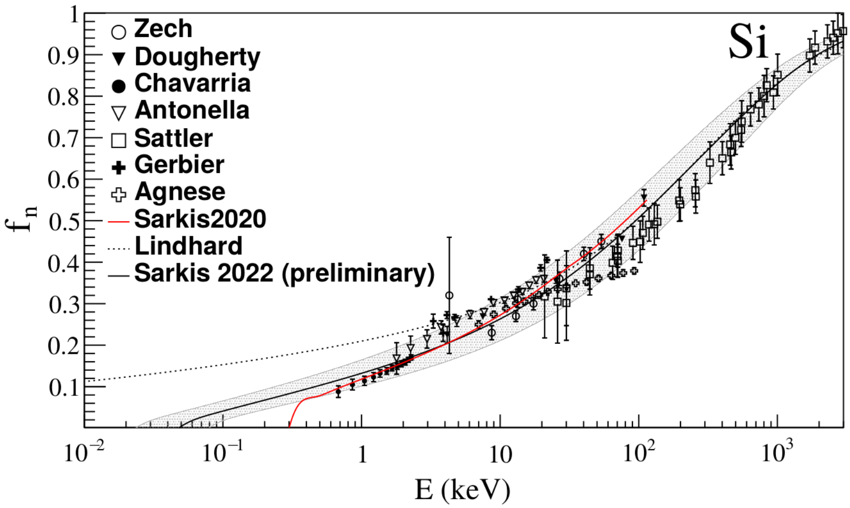

Results (Ge) with Collar recent data

For Ge study we have to consider a geometrical factor, mentioned by Tilinin and only significant for high Z ($Z > 20$).

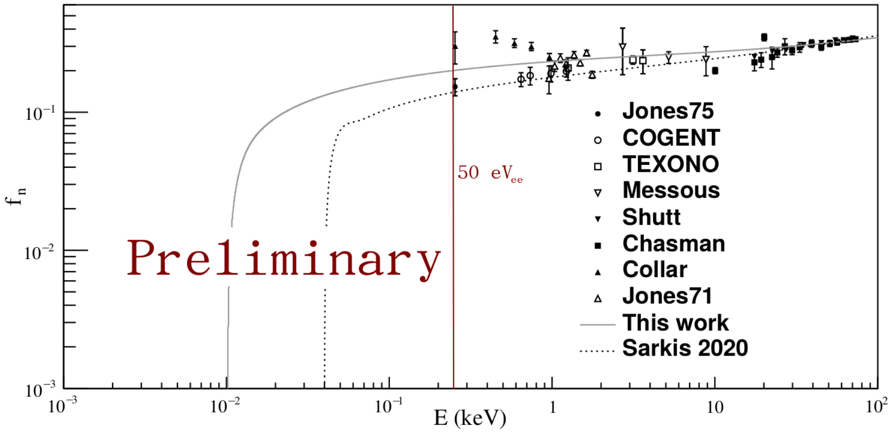

Figure: Germanium QF model with straggling, **geometrical factor**, low and high energy effects.

Noble Liquids Ionization Detectors; TPC's

TPC's

Combines the advantages of gas detectors: the possibility of proportional or EL amplification, XYZ positioning, and the possibility to have the large mass

TPC's were proposed by Russian scientists in 70's. And Dave Nygren in Lawrence Berkeley Lab.

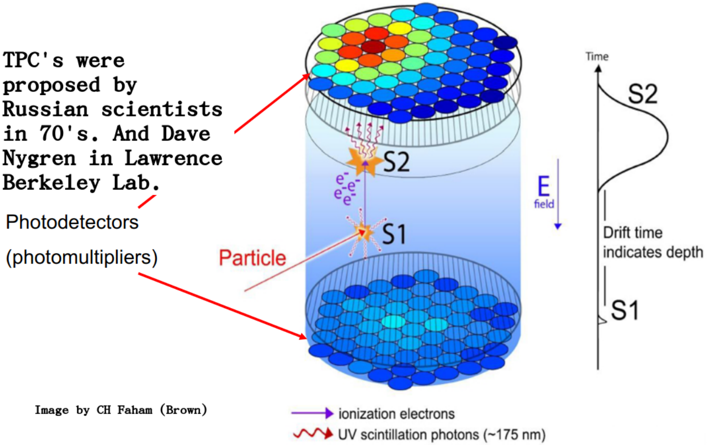

Image by CH Faham (Brown)

Noble Gases Ionization Response

- Dual-phase noble liquid time projection chambers (TPCs) have yielded, a competitive sensitivity for the search for WIMP's.
- Reconstruction is done by exploiting the full anticorrelation between the S1 (scintillation photons n_γ) and S2 (ionized electrons n_e).

$$E_{\text{er}} = W\left(\frac{S1}{g_1} + \frac{S2}{g_2}\right), \quad \to E_R = W\left(n_\gamma + n_e\right)/f_n,$$

- With $W_{Ar} = 19.5$ eV and $W_{Xe} = 13.7$ eV, is the average energy required to produce an excitation or ionization for Ar and Xe.
- A usual assumption is that each excited atom leads to one scintillation photon.
- And that each ionized atom leads to a single electron unless it recombines.

Thomas Imel Box Model

- Diffusion equation and separate ions-electrons recombination[10].

$$\frac{\partial N_+}{\partial t} = -\alpha N_- N_+,$$
$$\frac{\partial N_-}{\partial t} = u_- E \frac{\partial N_-}{\partial z} - \alpha N_+ N_-. \quad (9)$$

- We have $N_i + N_{ex} = n_\gamma + n_e$ independent of recombination.
- Assumes an initial condition,

$$N_0 = \begin{cases} \frac{N_i}{8a^3} & |x|,|y|,|z| < a \\ 0 & \text{otherwise} \end{cases} \quad (10)$$

- But this is just justifiable for MeV energies.
- The fraction of ionizations is predicted is

$$\frac{n_e}{N_i} = \frac{1}{\xi}\ln(1+\xi), \quad 1 - r = \frac{1}{\xi}\ln\left(1+\xi\right), \quad \xi = \frac{N_i \alpha}{4a^2 v}$$

[10] Ann.Phys.IV, V42, pp.303–344, (1913). PRA 36, 614 (1987)

Thomas Imel Low Energy Improvements

- Since Thomas-Imel model can be solved exactly, we can add diffusion as a perturbation,

$$1 - r = \frac{1}{\xi} \ln (1 + \xi) (1 + d_1 \xi^2 + d_2 \xi^4) \quad \text{Preliminary.}$$

- By also adding the bi-excitonic effect $k(N^+)^2$, we can explain Penning effects for light yield at high energies.
- For low energies the depth may not be well described by a constant distribution (box model).
- We can used both, S_e and S_n to model the initial distribution (work in progress).

Exciton-Ion Behavior

- Exciton to ion fraction $\beta = \frac{N_{ex}}{N_i}$ usually is modeled by a constant.
- With our formalism, we can built an Int.Diff. equation taking in to account the excitation and ionization cross sections (work in progress).
- A preliminary study justify that $\frac{N_{ex}}{N_i}$ changes slowly for energies > 1 keV.
- So if the total quanta $N_i + N_{ex} = N$ with $N = E_{er}/W$, hence $E_{er} = WN_i(1+\beta)$.
- If $N_{er} = f_n E_R$ then, $N_i = f_n(\frac{E_R}{W(1+\alpha)})$, where f_n can be computed with our model. spatially small tracks.

- In the following we show the Charge and Light Yiels for Ar and Xe, using the constant binding energy model and $S_e = k\varepsilon^{1/2}$.
- Where also we are taking β and $\frac{\alpha}{4a^2v} \equiv \gamma$ as constants.

Xenon Charge Yield

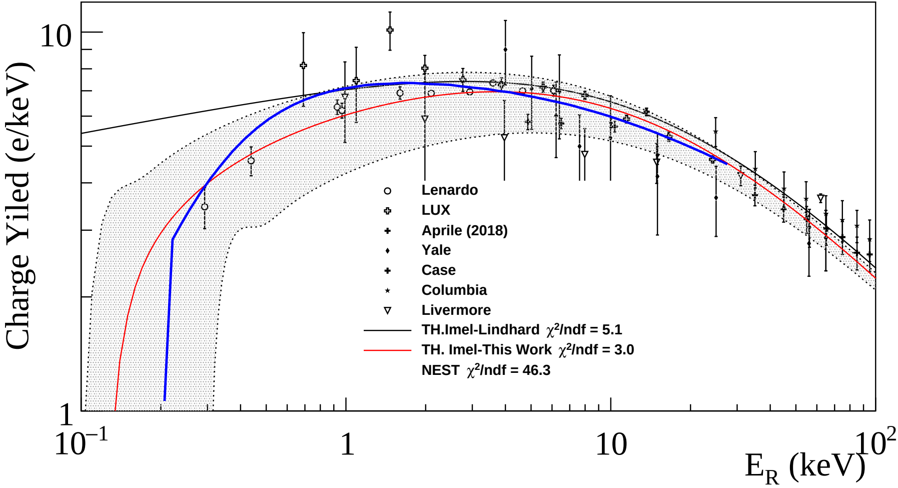

Figure: Charge Yield for Xe; $N_{ext}/N_i = 0.42$ and $\gamma = 0.015$

Xenon Light Yield

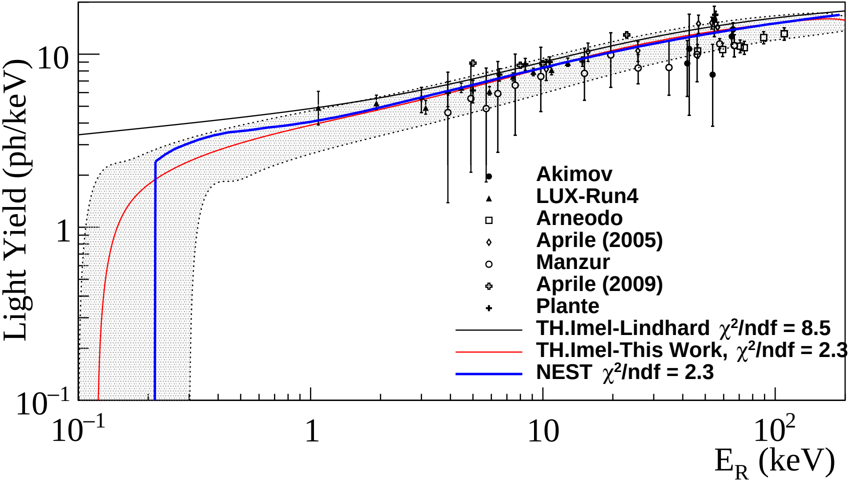

Figure: Light Yield for Xe; $N_{ext}/N_i = 0.42$ and $\gamma = 0.015$

Argon Charge Yield

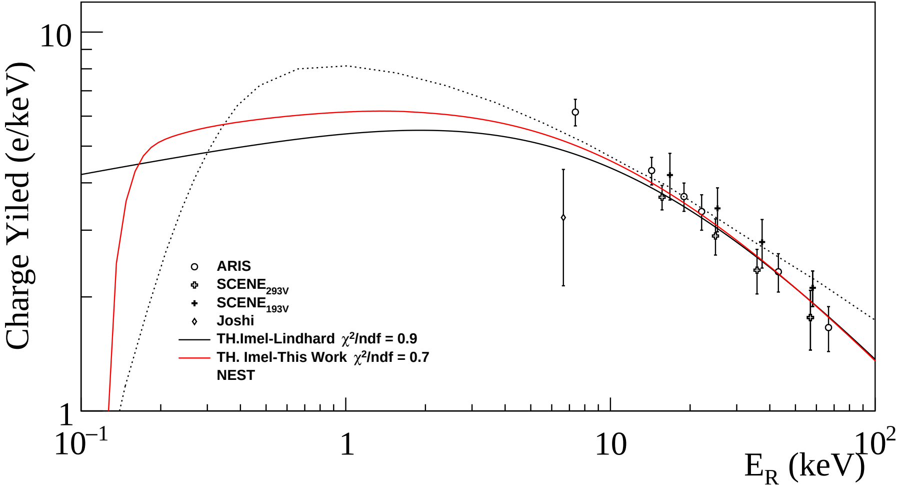

Figure: Charge Yield for Xe; $N_{ext}/N_i = 1.04$ and $\gamma = 0.030$

Argon Light Yield

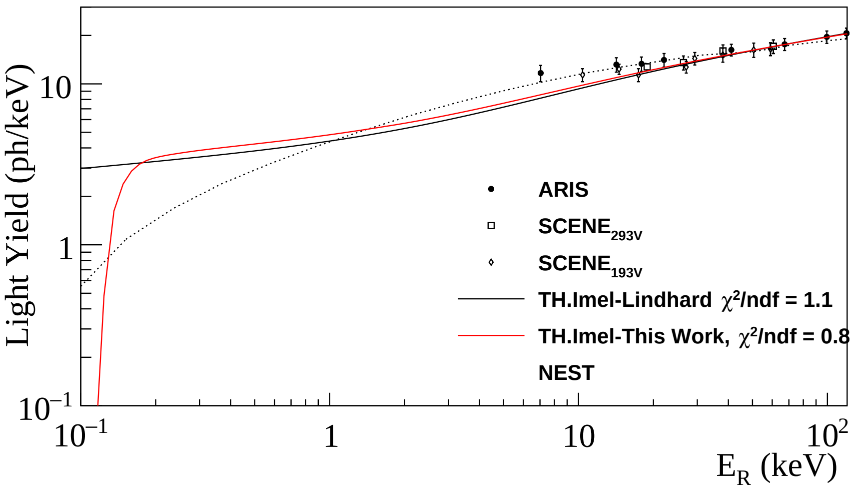

Figure: Light Yield for Xe; $N_{ext}/N_i = 1.04$ and $\gamma = 0.030$

Integral Equations; Other Applications.

Energy loss by defect creation in Si[11]

- Frenkel pairs (Fr-P) can create peak signals near threshold.
- We can compute the number of Fr-P by using Kinchin and Pease model combined with our solution for $\bar{\nu}$; $N_{Fr-P} = 0.8\bar{\nu}/2u_{Fr}$.

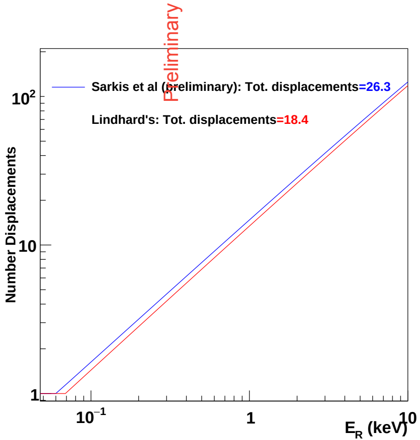

[11] Maitland Bowen and Patrick Huber, Phys.Rev.D 102, 053008 (2020)

EXCESS for Flat Low Energy Signals

- We can expect an EXCESS from a flat spectrum signal,.e.g. thermal Neutrons.
- By comparing spectrum reconstruction from Lindhard QF and our new QF model.
- Lindhard QF is usually used by MC simulations, etc.

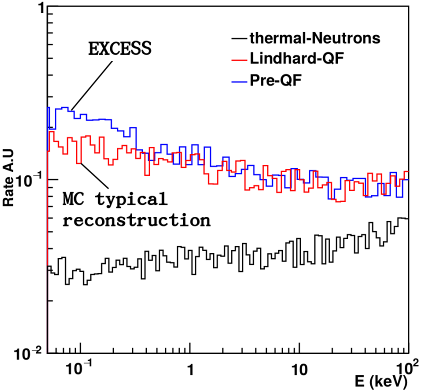

Jet Quenching (speculative idea)

- Lindhard integral equation can also be applied jet quenching for p+Pb.
- Since there is a competition between elastic and inelastic parton energy loss.
- The observable is the nuclear modification factor,

$$R_{\mathrm{pPb}} = \frac{d^2N_{\mathrm{pPb}}/dndp_{\mathrm{T}}}{\langle N_{\mathrm{coll}} > d^2N_{\mathrm{pp}}/dndp_{\mathrm{T}}} \qquad (11)$$

- That has been investigated in many theoretical studies on jets.

EPJ 182, 02126 (2018)

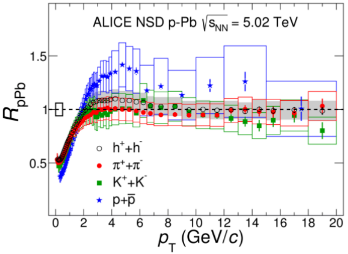

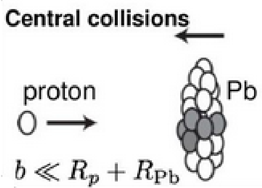

Credit: Hadron production in p-Pb collisions at LHCf,Albert Gamache

Conclusions

Conclusions

1. *We have presented the importance of the challenge for understanding ionization efficiency at low energies.*
2. *We present a general model based on integral equations for ionization in pure crystals and noble liquids.*
3. *We incorporate corrections due to electronic straggling and atomic scaling in the Int. Diff. Eq.*
4. *For silicon Coulomb effects allow us to fit the data up to 3 MeV and have a threshold near Frenkel-pair creation energy.*
5. *For germanium our model shows potential to explain recent measurements* [12].

[12] J.I.Collar, et al, PRD 103,122003 (2021)

Conclusions

- *We have shown the capacity of our model to explain charge and light yields in noble elements.*
- *We discuss important improvements at low energies, that can be added to Thomas Imel Box model.*
- *We have shown charge and light yields for Xe and Ar consistent with actual data.*
- *Much work can be done from here, e.g directional quenching factor, straggling for $\bar{\nu}$, etc.*

Thank You!

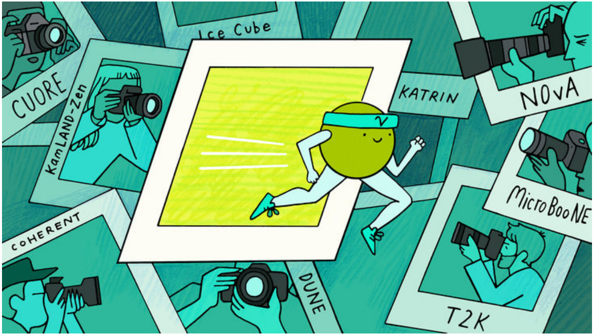

Illustration by Sandbox Studio, Chicago with Corinne Mucha

youssef@ciencias.unam.mx

❈ *This research was supported in part by DGAPA-UNAM grant number PAPIIT-IT100420, and Consejo Nacional de Ciencia y Tecnología (CONACYT) through gran CB2014/240666.*